Modern Particle Physics Experiments
Calorimeters

Aleksander Filip Żarnecki

FACULTY OF PHYSICS
UNIVERSITY OF WARSAW

Lecture 05

April 1, 2022

Detector concepts

Depending on the particle type and application, particle detectors can be divided into three main classes:

- Tracking detectors
  Measure position/trajectory of charged particles,
  based on energy losses due to ionization or activation of material.
  We try to minimize particle interactions
  $\Rightarrow$ gaseous detectors or thin semiconductor layers (shortly)
- Calorimeters (today)
  Measure particle energy by absorbing it in the dense medium
  Interactions of high energy incident particle
  $\Rightarrow$ electromagnetic or hadronic cascade
- Particle identification detectors
  Use different processes to improve particle identification capabilities
  Cherenkov detectors, Transition radiation detectors, Time-Of-Flight ...

References

- Particle Physics Reference Library (vol.2)
  Review of the state of the art in detector physics and related data-taking technology (open access)

- PDG reviews:
  - Passage of particles through matter
  - Particle detectors at accelerators
  - Particle detectors for non-accelerator physics

Calorimeters

1. Silicon detectors
2. Electromagnetic cascade
3. Electromagnetic calorimeters
4. Hadronic calorimeters

Calorimeters

1. Silicon detectors
2. Electromagnetic cascade
3. Electromagnetic calorimeters
4. Hadronic calorimeters

Principle of operation

Semiconductor detectors are solid state ionization chambers. Absorbed energy forms electron-hole (e-h) pairs, which induce a signal current on electrodes when moving under an applied electric field.

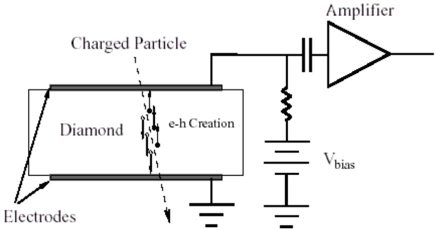

We typically use a p-n junction operated in reverse bias to form a larger sensitive region depleted of mobile charges.

Ionization losses in Silicon: $\frac{dE}{dx} \approx 3.88\, MeV/cm$

Energy required to create single e-h pair: $3.65\, eV$

$\Rightarrow$ about 100 e-h pairs per μm of depleted region ($\sim 1cm$ gas layer)

$\Rightarrow$ measurable charges already in $\mathcal{O}(100\mu m)$ Silicon layer

Applications

Semiconductor detectors provide outstanding detection opportunities in terms of energy, position and also time resolution.

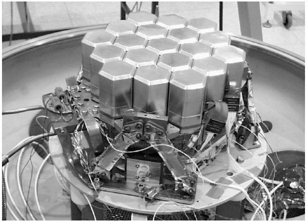

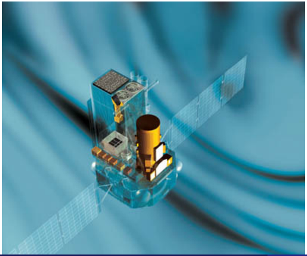

γ spectra from ITEGRAL detectors

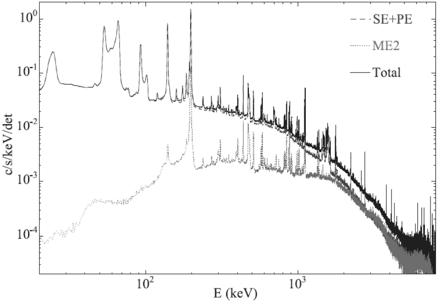

Total ionization in large Ge sensors measured. No position reconstruction...

Applications

In accelerator experiments most widely used as position sensitive devices

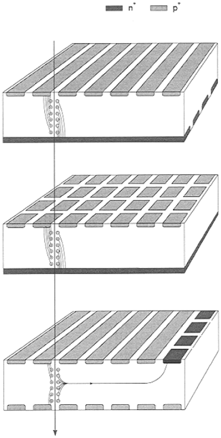

strip detector (1D)

also double sided ⇒

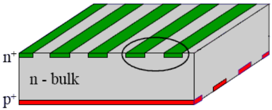

pixel detector (2D)

drift detector (2D) smaller number of channels

Technology choice

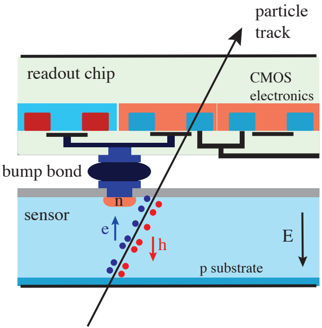

(a) Hybrid pixels

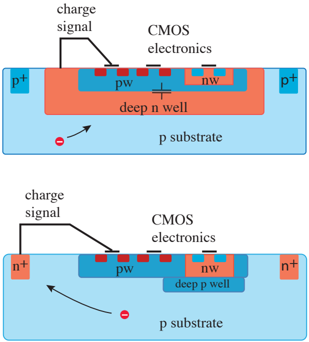

(b) Monolithic pixels

separate sensors and readout ICs connected by 2-D arrays of bumps

sensing and readout combined in one chip exploiting multi-well technology

Technology choice

Modern semiconductor detectors are strongly connected with integrated circuit technology ⇒ high-density micron-scale readout structures, high-density amplification and readout circuits.

Many different design principles possible:

- CCD (Charge-Coupled Device):
  high sensitivity, low noise, but very slow readout
- CP-CCD (Column Parallel CCD): faster readout possible
- MAPS (Monolithic active pixel sensors):
  on pixel amplification, fast readout, diffusion limited resolution
- DEPFET (DEPleted Field Effect Transistor):
  very thin sensors possible, high spacial resolution
- Timepix: combines precise arrival time and amplitude measurement (amplitude from TOT - time over threshold measurement)

Calorimeters

1 Silicon detectors

2 Electromagnetic cascade

3 Electromagnetic calorimeters

4 Hadronic calorimeters

Radiation losses

When interacting in matter charged particle can emit EM radiation

Emission probability:

$$p \sim \frac{1}{M^2}$$

$\Rightarrow$ important for lightest particles

Electron energy losses in lead as a function of energy

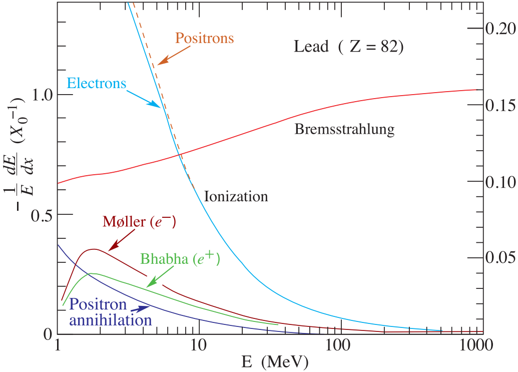

High energy electrons and positrons loose their energy mainly via radiation

Electromagnetic cascade

Radiation losses

Electron beam with initial energy of E_0 passing media of thickness x:

$$E(x) = E_0 \cdot \exp\left(-\frac{x}{X_0}\right)$$

X_0 - radiation length in given material. Approximate formula:

$$X_0 = \frac{A \cdot 716.4 \frac{g}{cm^2}}{Z(Z+1)\ln(287/\sqrt{Z})}$$

Decreasing fast with Z !

${}_{13}Al$: 8.9 cm, ${}_{26}Fe$: 1.76 cm

${}_{29}Cu$: 1.43 cm, ${}_{82}Pb$: 0.56 cm

Photon energy distribution: $y = \frac{E_\gamma}{E_0}$

$$\frac{d\sigma}{dE_\gamma} = \frac{A}{X_0 N_A E_\gamma}\left(\frac{4}{3} - \frac{4}{3}y + y^2\right)$$

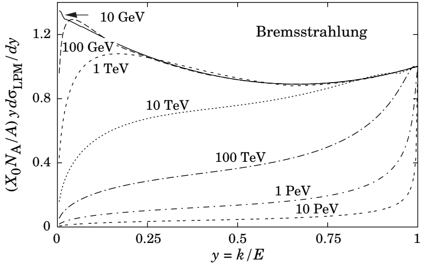

Deviations for most energetic electrons: radiation gets “harder”

Critical energy crucial parameter in cascade description

Energy for which radiative losses become higher than ionization losses in given medium

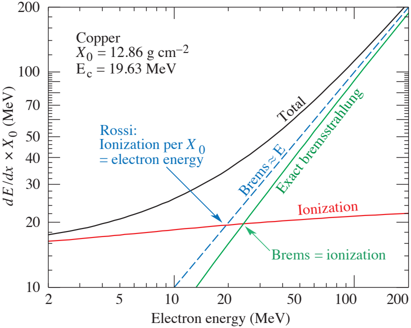

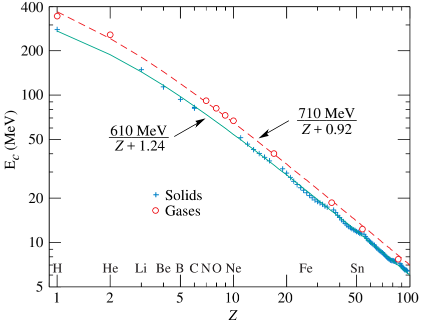

Critical energy E_c decreases fast with Z (similar to X_0)

Above E_c particle energy loss in medium is dominated by radiation

Electromagnetic cascade

Photon interactions

Photon interaction cross sections in carbon and lead

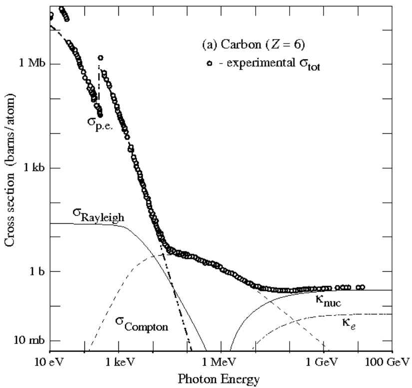

Photoelectric effect dominating at low energies ($\sigma_{p.e.}$)

For energies around 1 MeV - Comptona effect important ($\sigma_{Compton}$)

Above $\sim$ 10 MeV e^+e^- pair creation in the nucleus field dominates (κ_{nuc})

Pair creation

Probability for photon conversion into e^+e^- pair

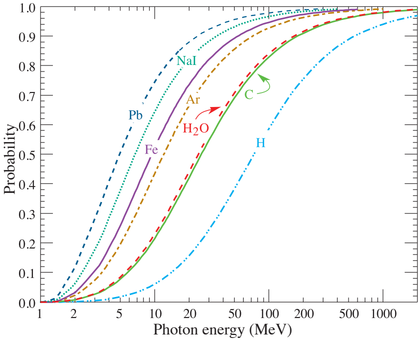

Above $\sim 1\ GeV$:
pair creation dominates

For lower energies, conversion contribution increases with Z

Absorption length for photons

Decrease of γ beam intensity

$$I(x) = I_0 \cdot \exp\left(-\frac{x}{\lambda}\right)$$

λ - interaction length

$$\lambda = \frac{1}{\sigma_{tot}} \cdot \frac{1}{n_a}$$

n_a - atomic density

$$n_a = \frac{N_A\ \rho}{A}$$

In high energy range $\gg E_c$ (pair creation dominates):

$$\lambda = \frac{9}{7} X_0$$

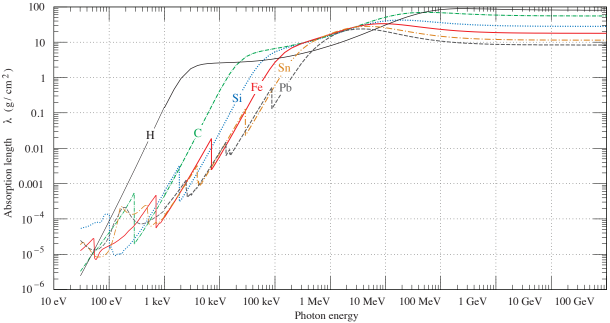

Cascade development

Above critical energy $E_c \sim 10 MeV$
photons convert to e^+e^- pairs

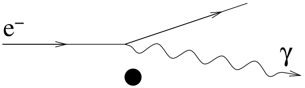

electrons loose their energy by
bremsstrahlung

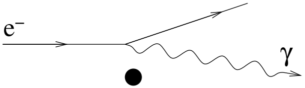

⇒ high energy electrons or photons create an electromagnetic cascade in dense media consisting of $N \sim E/E_c$ particles

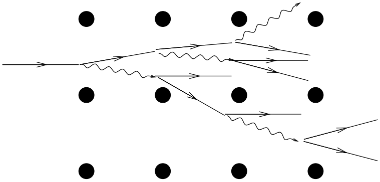

No energy loss in bremsstrahlung or pair creation
⇒ 100% deposited in ionization ⇒ precise energy measurement possible

Cascade simulation 05_em_shower.ipynb (1)

Simplified model:

- uniform energy sharing (both for conversion and bremsstrahlung)
- uniform ionization losses (independent on energy)
- cascade development stops when particle energy below E_c

Incident electron:
$E = 5\,\text{GeV}$

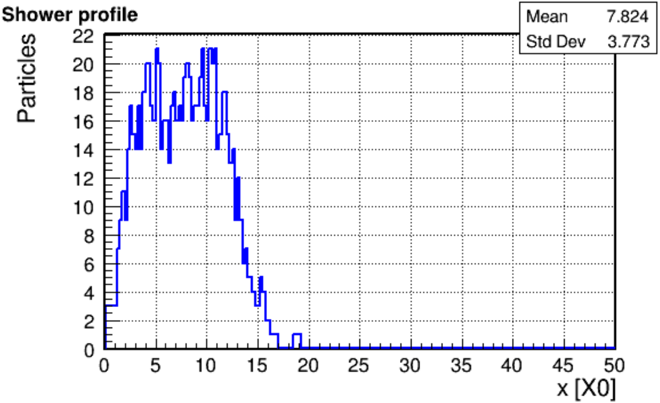

Cascade profile

Simulated shower profile averaged over 1000 generations

Incident electron:
$E = 1\,\mathrm{GeV}$

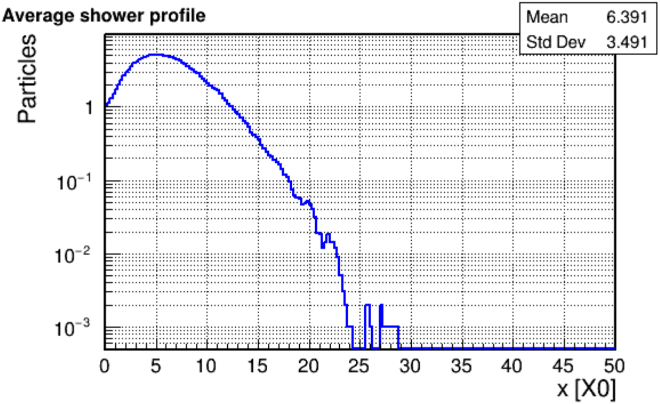

Cascade profile

Simulated shower profile averaged over 1000 generations

Incident electron:
E = 2 GeV

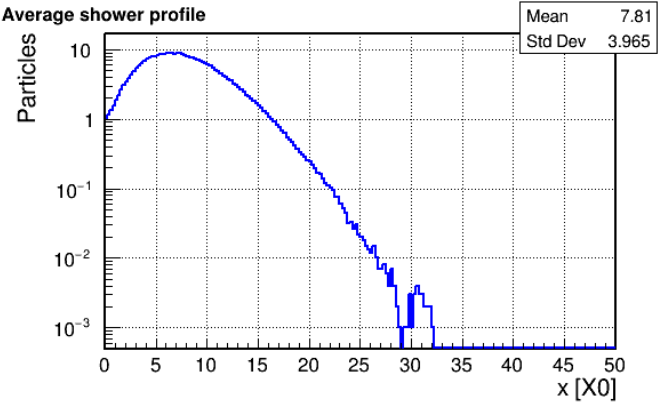

Cascade profile

Simulated shower profile averaged over 1000 generations

Incident electron:
$E = 3\,\text{GeV}$

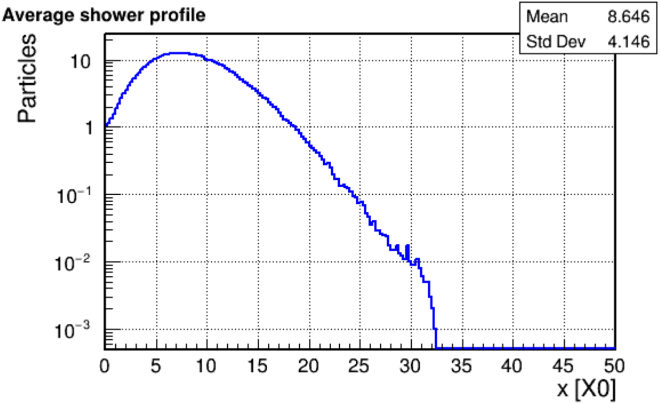

Cascade profile

Simulated shower profile averaged over 1000 generations

Incident electron:
E = 5 GeV

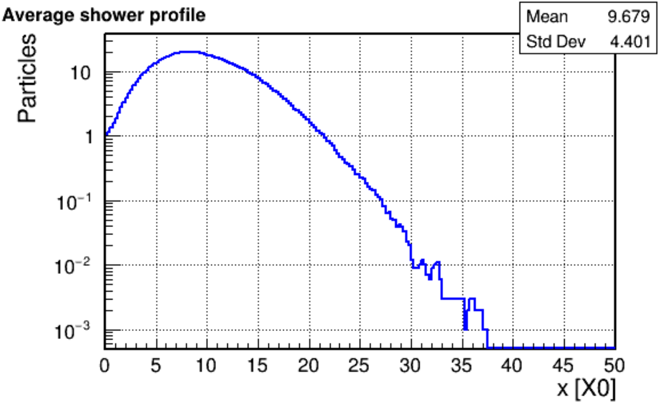

Cascade profile

Simulated shower profile averaged over 1000 generations

Incident electron:
$E = 10\,\mathrm{GeV}$

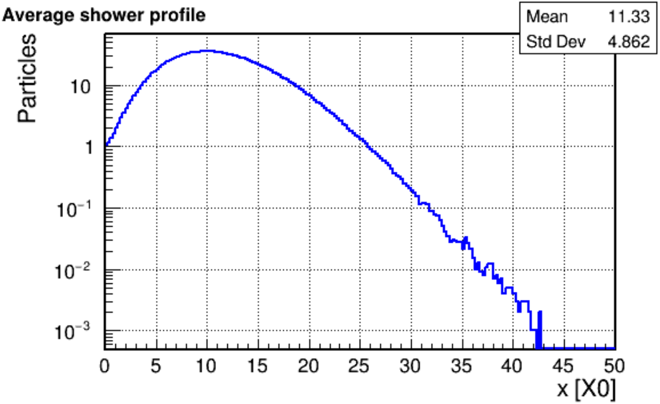

Cascade profile

Simulated shower profile averaged over 1000 generations

Incident electron:
E = 20 GeV

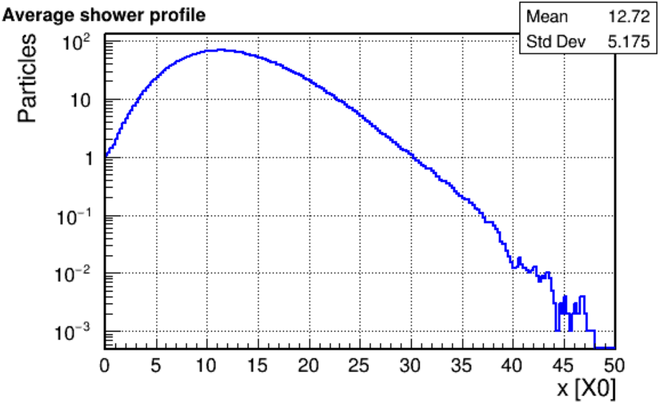

Maximum position and penetration depth increases with $\log(E)$

Cascade profile

Longitudinal EM shower profile well described by Gamma distribution

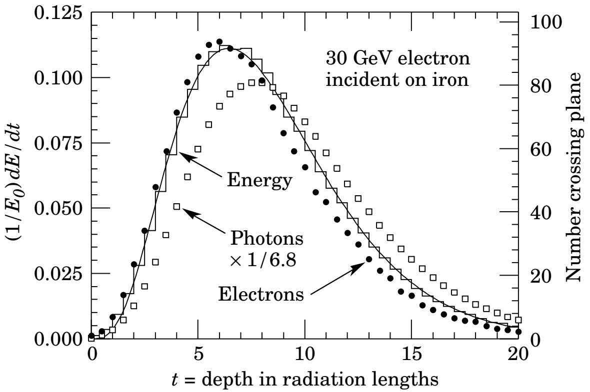

$$\frac{dE}{dt} = E_0 \; b \; \frac{(bt)^{a-1} \; e^{-bt}}{\Gamma(a)}$$

Maximum position

$$t_{max} = \frac{a-1}{b}$$

EM shower profile

Use the proposed shower development model to generate EM cascades for few incident electron energies (between 1 GeV and 100 GeV).

For each energy:

- find the maximum position of the average cascade profile
- find the calorimeter depth required to contain (on average) 99% of cascade energy

How do these two quantities depend on the incident electron energy?

Hint: equivalent form of Gamma function, more stable in numerical fitting

$$y(x) \quad = \quad y_0 \cdot \exp\left[-\left(\frac{x_0}{\sigma}\right)^2 \cdot \left(\frac{x - x_0}{x_0} - \ln\frac{x}{x_0}\right)\right]$$

x_0 - maximum position, y_0 - value at maximum, σ - width parameter

Calorimeters

1. Silicon detectors
2. Electromagnetic cascade
3. Electromagnetic calorimeters
4. Hadronic calorimeters

Calorimeter types

Different processes can be used to measure particle energy losses.
Two main options:

Uniform

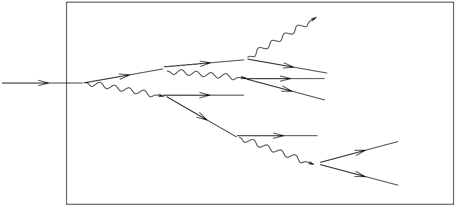

Cascade develops in sensitive media
⇒ total energy measured

Can be divided into segments
for better position readout

Sampling

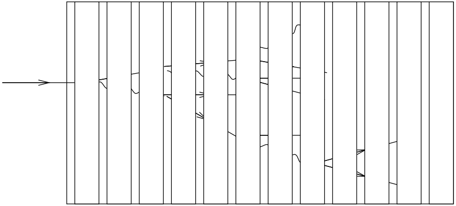

Cascade develops in dense absorber
interleaved with sensitive layers
⇒ only a fraction of energy measured
Smaller and cheaper, but the
measurement resolution can be worse

Uniform calorimeter 05_em_shower.ipynb (2)

Distribution of the total charged particle track length for 1000 cascades

Ionization $\sim$ total track length

Incident electron:
$E = 1\,\mathrm{GeV}$

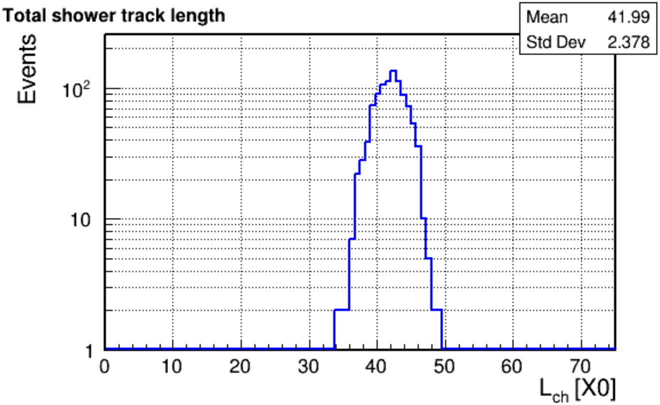

Uniform calorimeter 05_em_shower.ipynb (2)

Distribution of the total charged particle track length for 1000 cascades

Ionization $\sim$ total track length

Incident electron:
$E = 2\,\text{GeV}$

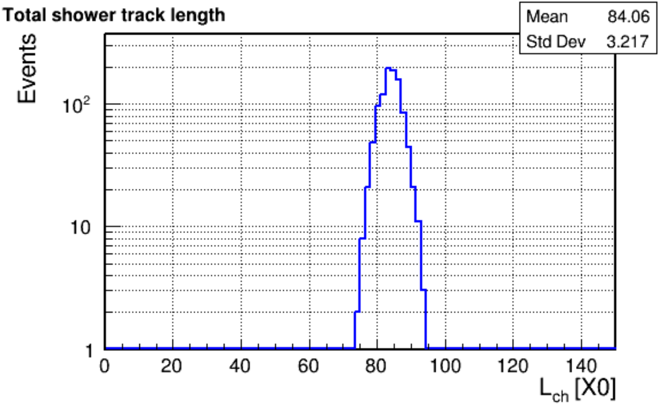

Uniform calorimeter 05_em_shower.ipynb (2)

Distribution of the total charged particle track length for 1000 cascades

Ionization $\sim$ total track length

Incident electron:

$E = 3\,\mathrm{GeV}$

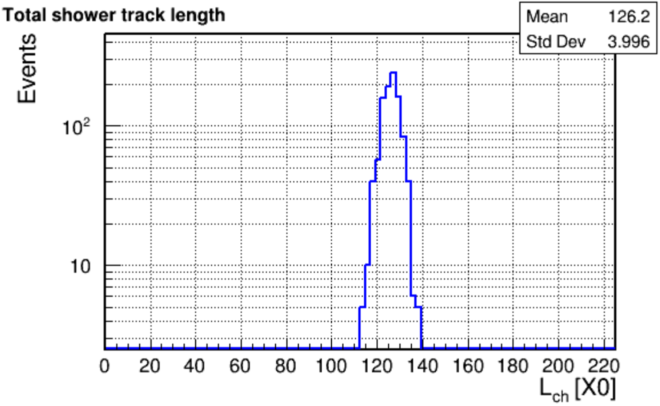

Uniform calorimeter 05_em_shower.ipynb (2)

Distribution of the total charged particle track length for 1000 cascades

Ionization $\sim$ total track length

Incident electron:

$E = 5\,\mathrm{GeV}$

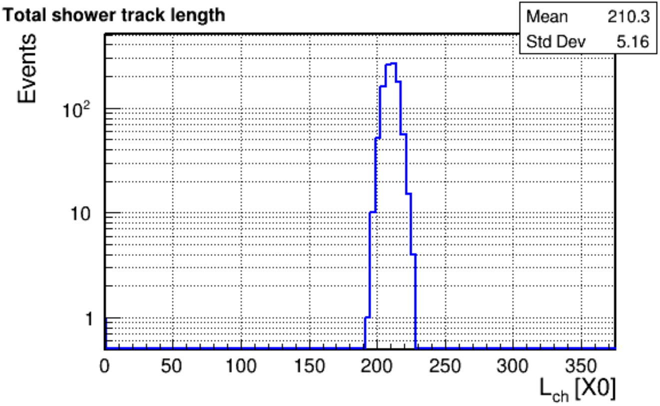

Uniform calorimeter 05_em_shower.ipynb (2)

Distribution of the total charged particle track length for 1000 cascades

Ionization $\sim$ total track length

Incident electron:

$E = 10\,\mathrm{GeV}$

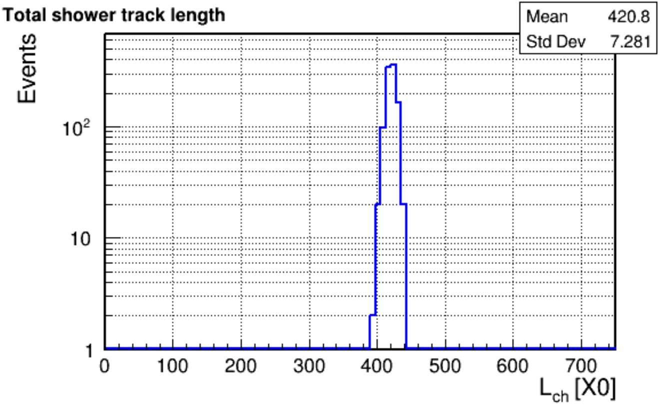

Uniform calorimeter 05_em_shower.ipynb (2)

Distribution of the total charged particle track length for 1000 cascades

Ionization $\sim$ total track length

Incident electron:

$E = 20\,\mathrm{GeV}$

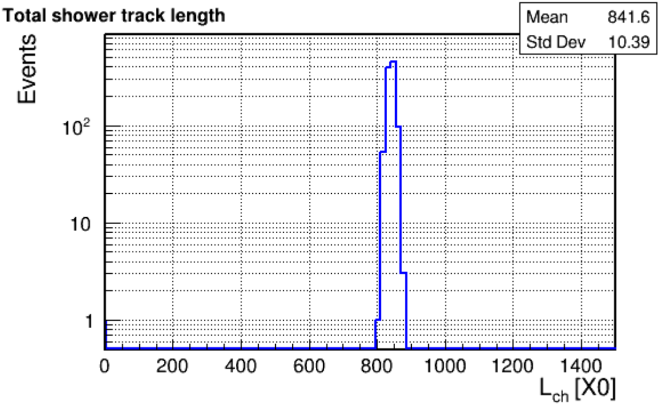

Total track length proportional to energy. Relative width decreases.

Energy resolution

Relative width of the track length distribution ⇒ energy resolution

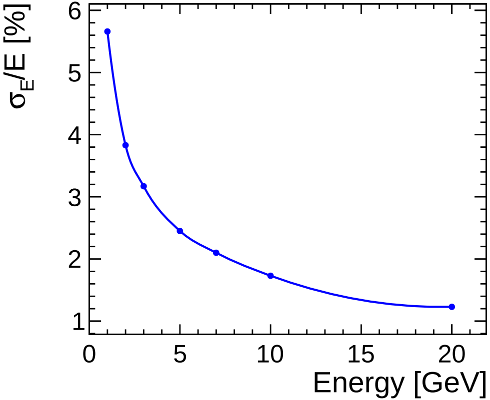

Energy resolution

Relative width of the track length distribution $\Rightarrow$ energy resolution

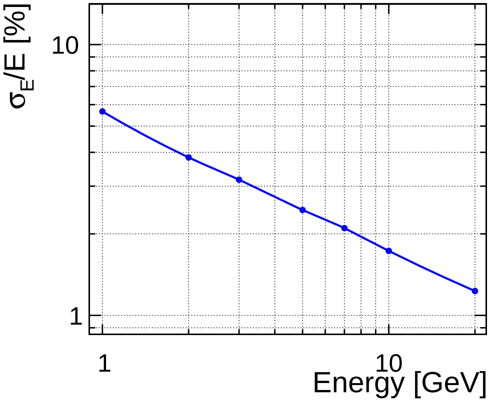

Energy resolution decreases as $1/\sqrt{E}$

Energy resolution

Relative width of the track length distribution $\Rightarrow$ energy resolution

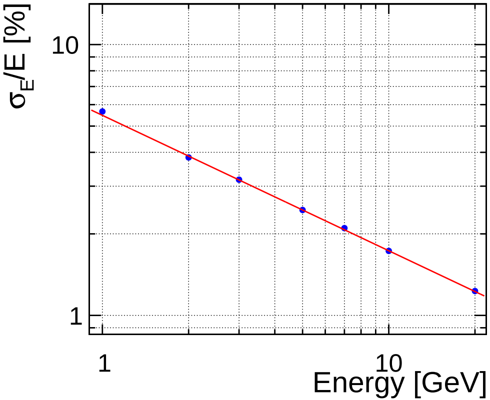

Energy resolution decreases as $1/\sqrt{E}$

Fit: $\sigma_E/E = 5.5\%/\sqrt{E}$

Sampling calorimeters

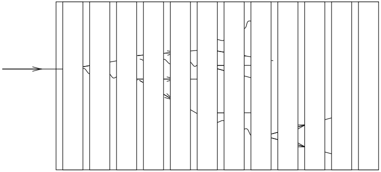

Cascade develops in dense absorber interleaved with sensitive layers

Advantages:

- smaller, very dense absorber can be used
- cheaper, absorber is much cheaper than readout elements
- more options for optimisation (eg. segmentation)
- can be used for both electromagnetic and hadronic cascades

Disadvantages:

- lower signal, noise can be a problem
- worse resolution

Sampling calorimeter 05_em_shower.ipynb (3)

Assume very thin sensitive layers ⇒ counting charged particles

Results for 1 X_0 sampling length

Incident electron:
E = 2 GeV

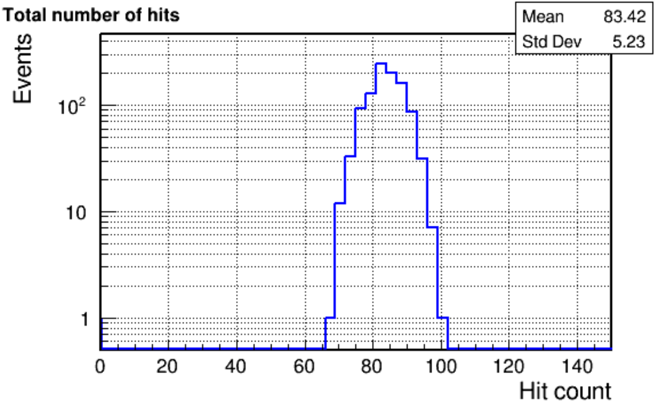

Sampling calorimeter 05_em_shower.ipynb (3)

Assume very thin sensitive layers $\Rightarrow$ counting charged particles

Results for 1 X_0 sampling length

Incident electron:

E = 5 GeV

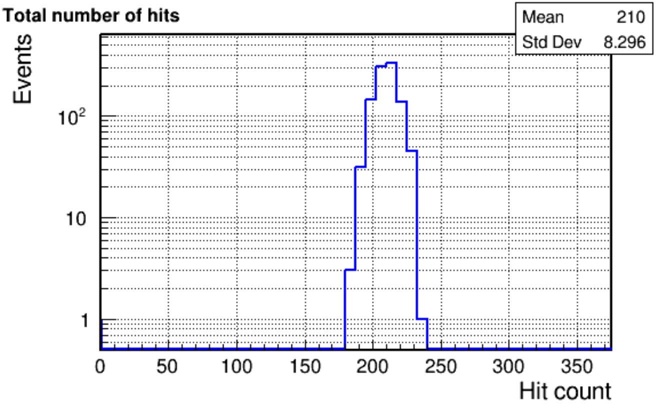

Sampling calorimeter 05_em_shower.ipynb (3)

Assume very thin sensitive layers $\Rightarrow$ counting charged particles

Results for 1 X_0 sampling length

Incident electron:
E = 20 GeV

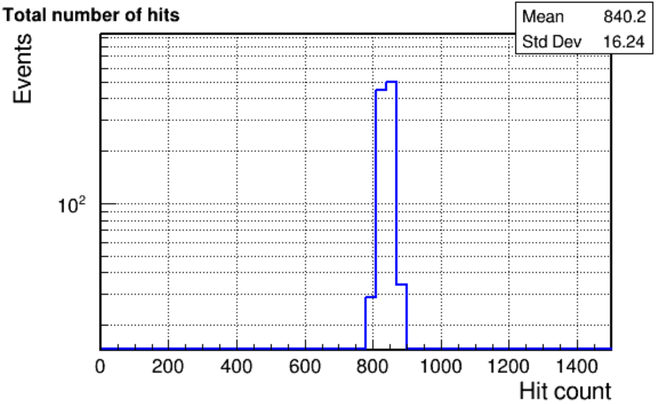

Response still linear!

Sampling calorimeter

Resolution of the sampling calorimeter at 5 GeV vs the uniform one

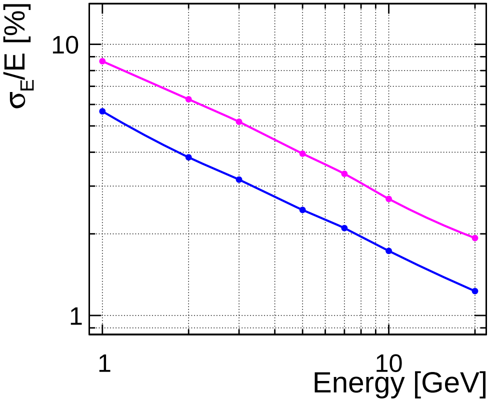

Follows same energy dependence: $\sim 1/\sqrt{E}$

Sampling calorimeter 05_em_shower.ipynb (4)

Assume very thin sensitive layers $\Rightarrow$ counting charged particles

Results incident electron energy of 5 GeV

Sampling length:

$\Delta = 0.2\,X_0$

$\sigma/E = 2.43\%$

2.35% for uniform

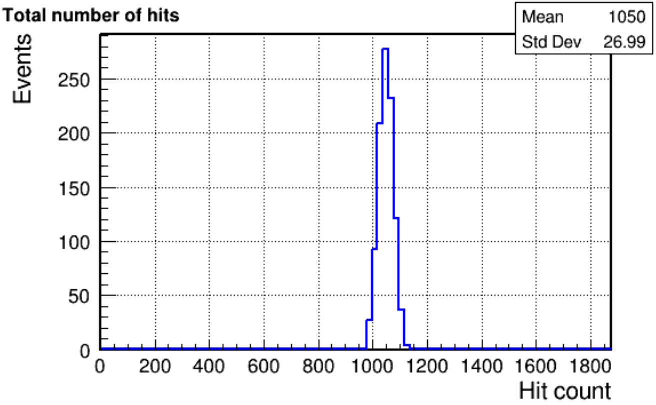

Sampling calorimeter 05_em_shower.ipynb (4)

Assume very thin sensitive layers ⇒ counting charged particles

Results incident electron energy of 5 GeV

Sampling length:

$\Delta = 0.5\,X_0$

$\sigma/E = 2.76\%$

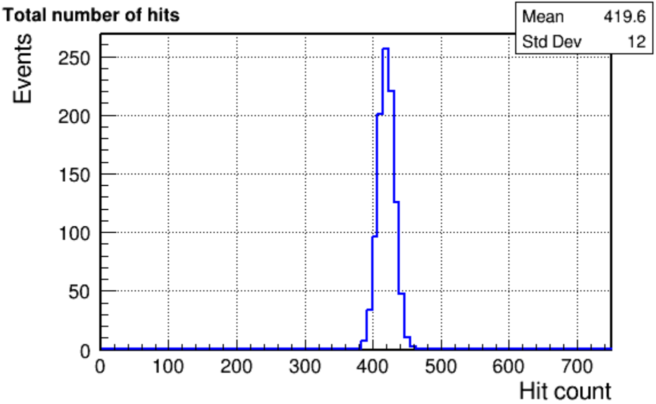

Electromagnetic calorimeters

Sampling calorimeter 05_em_shower.ipynb (4)

Assume very thin sensitive layers ⇒ counting charged particles

Results incident electron energy of 5 GeV

Sampling length:

$\Delta = 1\,X_0$

$\sigma/E = 3.83\%$

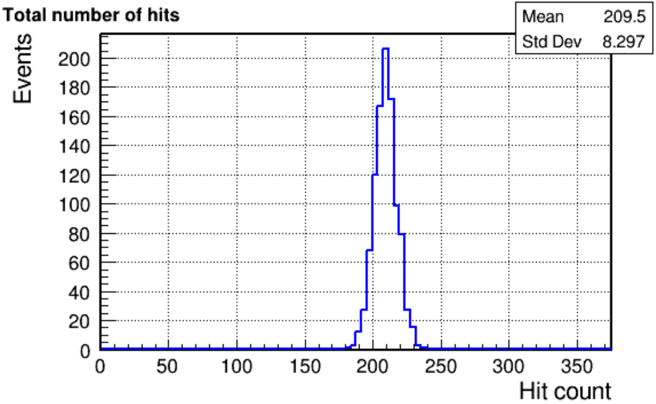

Resolution worsen with increasing sampling length

Sampling calorimeter 05_em_shower.ipynb (4)

Assume very thin sensitive layers ⇒ counting charged particles

Results incident electron energy of 5 GeV

Sampling length:

$\Delta = 2\,X_0$

$\sigma/E = 6.20\%$

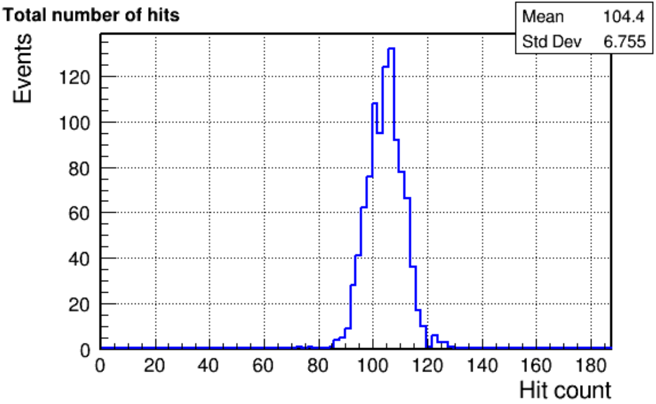

Resolution worsen with increasing sampling length

Sampling calorimeter 05_em_shower.ipynb (4)

Assume very thin sensitive layers $\Rightarrow$ counting charged particles

Results incident electron energy of 5 GeV

Sampling length:

$\Delta = 4\,X_0$

$\sigma/E = 10.7\%$

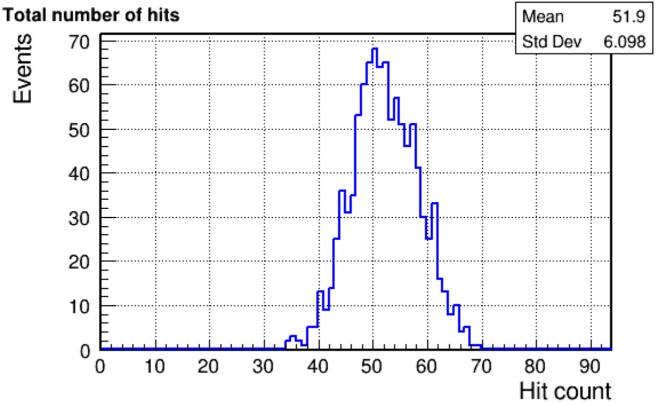

Resolution worsen with increasing sampling length

Sampling calorimeter

Resolution of the sampling calorimeter at 5 GeV

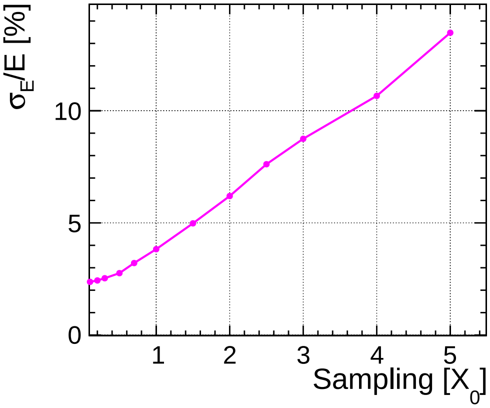

Resolution worsens fast with increasing sampling length...

Energy resolution

General formula for the calorimeter energy resolution:

$$\frac{\sigma_E}{E} = \frac{a}{\sqrt{E}} \oplus \frac{b}{E} \oplus c$$

where subsequent terms reflect

- a: statistical fluctuations in cascade development (and sampling)
  $N \sim E \;\Rightarrow\; \sigma_N = \sqrt{N} \;\Rightarrow\; \sigma_E \sim \sqrt{E}$
- b: detector and electronics noise
- c: nonuniformities, nonlinear response, channel calibration errors, cascade leakages   dominates at large energies

$$a \oplus b \equiv \sqrt{a^2 + b^2}$$

Energy resolution

Resolution of typical electromagnetic calorimeters   E is in GeV

Technology (Experiment)	Depth	Energy resolution	Date
NaI(Tl) (Crystal Ball)	$20X_0$	$2.7\%/\mathrm{E}^{1/4}$	1983
$Bi_4Ge_3O_{12}$ (BGO) (L3)	$22X_0$	$2\%/\sqrt{E} \oplus 0.7\%$	1993
CsI (KTeV)	$27X_0$	$2\%/\sqrt{E} \oplus 0.45\%$	1996
CsI(Tl) (BaBar)	16–$18X_0$	$2.3\%/E^{1/4} \oplus 1.4\%$	1999
CsI(Tl) (BELLE)	$16X_0$	1.7% for $E_\gamma > 3.5$ GeV	1998
CsI(Tl) (BES III)	$15X_0$	2.5% for $E_\gamma = 1$ GeV	2010
$PbWO_4$ (PWO) (CMS)	$25X_0$	$3\%/\sqrt{E} \oplus 0.5\% \oplus 0.2/E$	1997
$PbWO_4$ (PWO) (ALICE)	$19X_0$	$3.6\%/\sqrt{E} \oplus 1.2\%$	2008
Lead glass (OPAL)	$20.5X_0$	$5\%/\sqrt{E}$	1990
Liquid Kr (NA48)	$27X_0$	$3.2\%/\sqrt{E} \oplus 0.42\% \oplus 0.09/E$	1998
Scintillator/depleted U (ZEUS)	20–$30X_0$	$18\%/\sqrt{E}$	1988
Scintillator/Pb (CDF)	$18X_0$	$13.5\%/\sqrt{E}$	1988
Scintillator fiber/Pb spaghetti (KLOE)	$15X_0$	$5.7\%/\sqrt{E} \oplus 0.6\%$	1995
Liquid Ar/Pb (NA31)	$27X_0$	$7.5\%/\sqrt{E} \oplus 0.5\% \oplus 0.1/E$	1988
Liquid Ar/Pb (SLD)	$21X_0$	$8\%/\sqrt{E}$	1993
Liquid Ar/Pb (H1)	20–$30X_0$	$12\%/\sqrt{E} \oplus 1\%$	1998
Liquid Ar/depl. U (DØ)	$20.5X_0$	$16\%/\sqrt{E} \oplus 0.3\% \oplus 0.3/E$	1993
Liquid Ar/Pb accordion (ATLAS)	$25X_0$	$10\%/\sqrt{E} \oplus 0.4\% \oplus 0.3/E$	1996

Calorimeters

1 Silicon detectors

2 Electromagnetic cascade

3 Electromagnetic calorimeters

4 Hadronic calorimeters

Hadron interactions

Cross section for elastic hadron scattering decreases fast with energy.

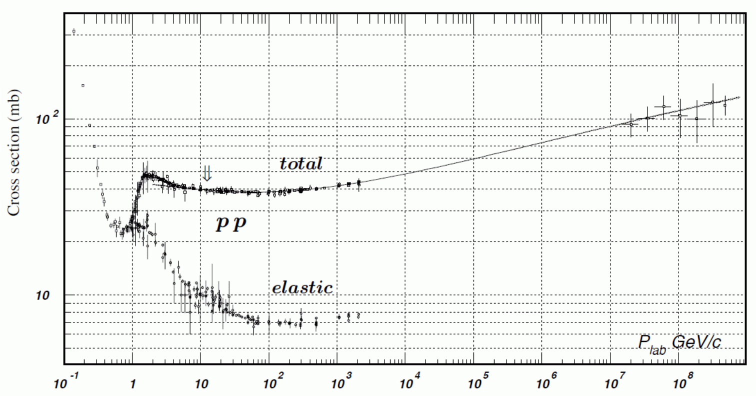

For energies above few GeV, inelastic scattering dominates,
cross section dependence on energy is very weak (note plot range)

Interaction length

Inelastic scattering probability as a function of material depth:

$$p(x) = \frac{1}{\lambda_I} \cdot \exp\left(-\frac{x}{\lambda_I}\right)$$

λ_I - nuclear interaction length

$$\lambda_I \approx 35\ g/cm^2\ A^{1/3}$$

	λ_I	X_0	λ_I/X_0
$_{13}Al$	39.4 cm	8.9 cm	4
$_{26}Fe$	16.8 cm	1.76 cm	10
$_{29}Cu$	15.1 cm	1.43 cm	11
$_{82}Pb$	17.1 cm	0.56 cm	30

Average interaction length decreases with Z, but slower than X_0

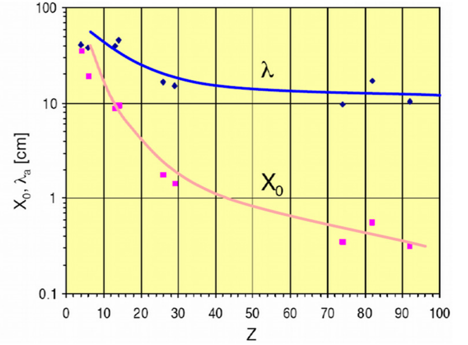

$\Rightarrow$ hadronic cascades develop slower and are much longer than EM ones

Hadronic cascade

High energy hadrons (charged and neutral) interact with nucleons or nuclei in the media, secondary particles are produced. $N \sim \ln E$

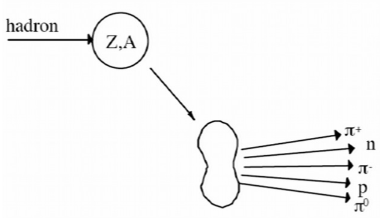

Secondary particles create more particles in subsequent interactions
$\Rightarrow$ hadronic cascade

Particles loose energy in ionization and nuclear excitations
π° decays $\Rightarrow$ EM component

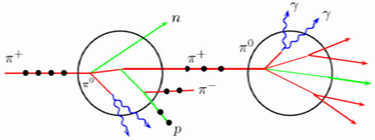

Excitations $\Rightarrow$ delay particle emission

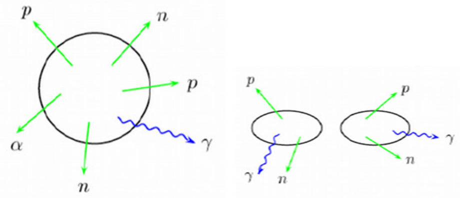

Hadronic cascade

Cascade profile scales with λ_I:

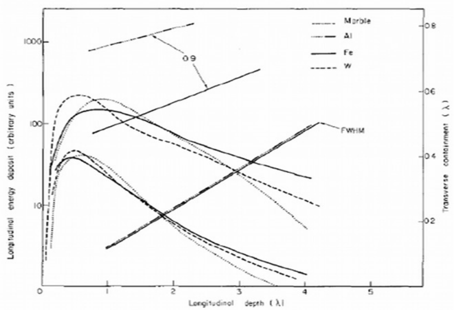

Maximum position $[\lambda_I]$:

$$t_{max} \approx 0.2 \ln E[GeV] + 0.7$$

Iron depth required to “stop” the cascade: (95% or 99% of energy)

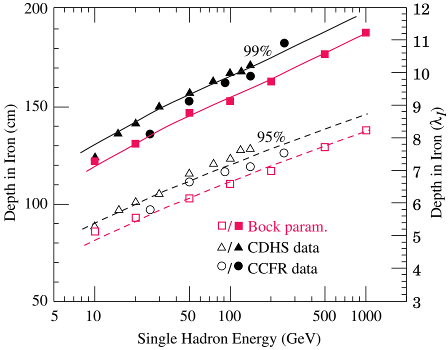

Required depth rises with $\log(E)$

Energy resolution

About half of the hadronic cascade energy is deposited via EM component (mainly due to π^0 production)

Most calorimeters: different response to EM component and to hadrons!

- large fluctuations of EM faction limit energy resolution!
- average EM contribution increasing with energy $\Rightarrow$ nonlinearity

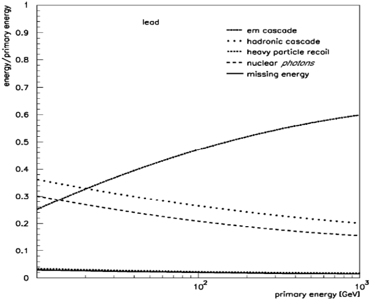

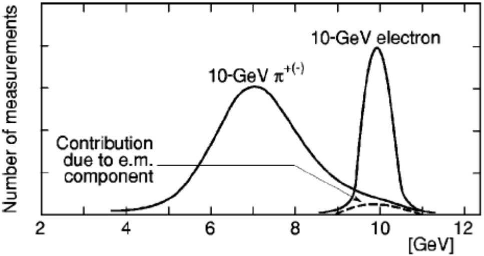

Signal (in energy units) obtained for a 10 GeV energy deposit

Energy resolution

Energy resolution for selected collider experiments
combined electromagnetic and hadronic calorimeter systems

Experiment	technology (ECAL, HCAL)	Combined hadronic resolution
H1	Pb/LAr, Steel / LAr	$46\%/\sqrt{E} \oplus 2.6\% \oplus 0.73/E$
ZEUS	depleted U / plastic scintillator	$35\%/\sqrt{E}$
CDF	Pb/plastic scint., Steel/plastic scint.	$68\%/\sqrt{E} \oplus 4.1\%$
D0	depleted U / LAr	$44.6\%/\sqrt{E} \oplus 3.9\%$
ATLAS	Pb/LAr, Steel/plastic scintillator	$52\%/\sqrt{E} \oplus 3.0\% \oplus 1.6/E$
CMS	$PbWO_4$, brass/plastic scintillator	$84.7\%/\sqrt{E} \oplus 7.4\%$

PDG compilation of results for single hadrons taken from beam tests of prototypes

Energy resolution for hadronic cascade much worse than for EM one

Is there anything we can do about it?

How to improve jet energy resolution?

crucial for collider experiments

Different approaches possible:

- hardware compensation: design calorimeter in such a way, as to obtain same response to electrons and hadrons
- software compensation: reconstruct EM fraction from cascade profile and correct the measurement
- dual readout: allows to extract EM and hadronic components
- particle flow reconstruction: avoid hadronic component measurement

Hardware compensation example of ZEUS experiment at HERA

Very dense absorber (uranium) and very light sensitive material (organic scintillator)

- higher sensitive volume fraction for hadronic part
- organic scintillator sensitive to neutrons from uranium fission (recover part of nuclear losses)

Final design based on prototype tests

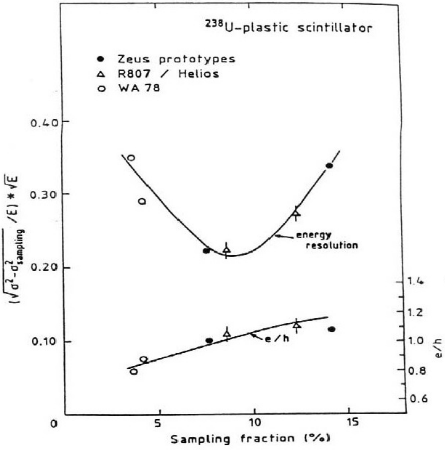

Software compensation

Hardware compensation is expensive.
Also results in poor EM resolution.

However, with high readout segmentation one can try to reconstruct EM component fraction f_{em} on event-by-event basis and extract energy E from the measurement:

$$E_{meas} \quad = \quad (f_{em} + \eta_{had}(1 - f_{em})) \cdot E$$

where: η_{had} - relative suppression of hadronic component (~ 0.7)

EM component visible as highly localized deposits ($X_0 \ll \lambda_{int}$)

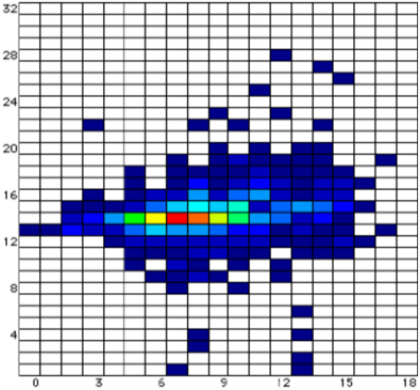

Hadronic calorimeters

Software compensation

First used in CDHSW Neutrino Experiment (WA1) at CERN (1976-1984)

EM fraction estimated from the maximum deposit in single cell

Significant improvement of energy resoultion, for high energies in particular
For single particles only

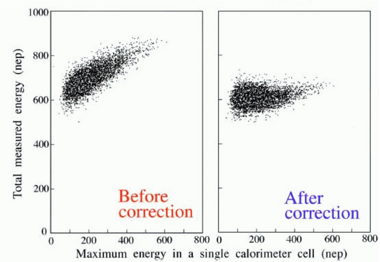

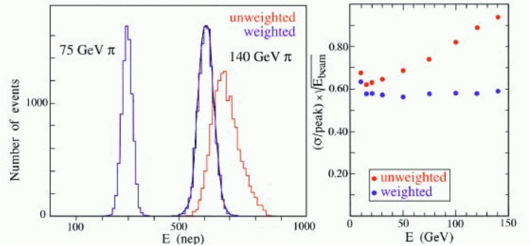

Dual readout

Two independent readouts, based on two different detection processes: scintillation and Cherenkov radiation.

$$E_{Sci} = (f_{em} + \eta_{Sci}(1 - f_{em})) \cdot E$$
$$E_{Ch} = (f_{em} + \eta_{Ch}(1 - f_{em})) \cdot E$$

As suppression factors are known:

$$\eta_{Sci} \approx 0.6$$
$$\eta_{Ch} \approx 0.25$$

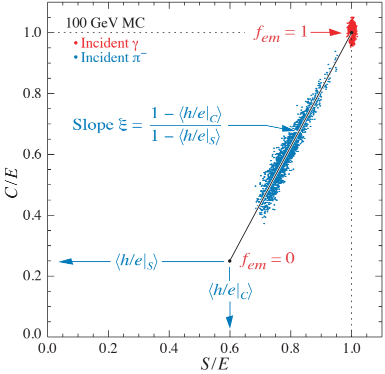

f_{em} and E can be extracted from the two measured signals
$\Rightarrow$ significantly improved energy resolution

Particle Flow

Jet energy resolution crucial for precision physics and background rejection

Typical jet composition:

- 60% charged particles
- 30% photons
- 10% neutral hadrons

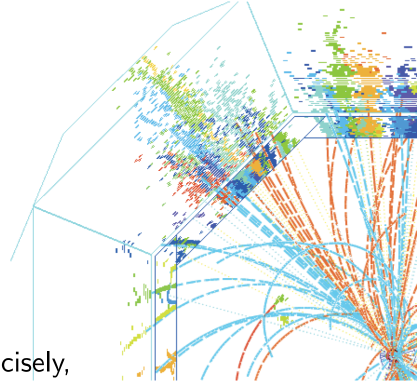

Jet energy poorly measured in calorimeters, large flactuations.

But we can measure:

- charged particle momenta very precisely,
- photon energy quite well,
- only neutral hadrons are a problem...

Particle Flow

Main concept:
try to measure jet energy
particle by particle

Very high granularity
for both EM and HAD calorimeters
$\Rightarrow$ single particle reconstruction/ID

- for charged particles (60%)
  best energy estimate from precise momentum measurement
- for photons (30%)
  precise measurement in ECAL
- only for neutral hadrons (10%)
  hadronic calorimeter has to be used

Example ILC event
$e^+e^- \rightarrow t\bar{t} \rightarrow 6j$

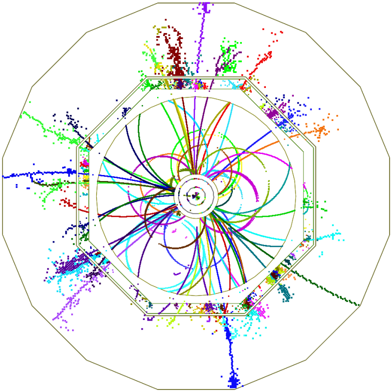

Particle Flow

Measurement of neutral hadrons, contributing around 10% to jet energy (on average, fluctuates a lot) gives dominant contribution to the jet energy resolution at low energies.

For high energies, the performance is dominated by "confusion term" (efficiency of particle separation)

3% jet energy resolution expected for light quark jets

ILD simulation results